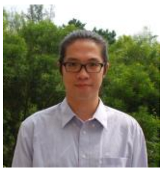

Kevin Ka-Lun Lau

# Determining the optimal size of local climate zones for spatial mapping in high-density cities

Kevin Ka-Lun Lau[1], Chao Ren[1], Yuan Shi[1], Venessa Zheng[1], Steve Yim[2,3], Derrick Lai[2,3]

[1] *School of Architecture, The Chinese University of Hong Kong, Hong Kong, kevinlau@cuhk.edu.hk*

[2] *Department of Geography and Resource Management, The Chinese University of Hong Kong, Hong Kong*

[3] *Centre for Environmental Policy and Resource Management, The Chinese University of Hong Kong, Hong Kong*

## 1. Introduction

Urbanization involves the conversion of rural land into urban settlements and alters its original surface characteristics, resulting in distinctive climatic conditions in urban areas (Oke, 1982; 1987). Such an altered climate leads to the formation of urban heat island (UHI) phenomenon (Giridharan et al., 2004; Lau et al., 2011) and associated impacts on thermal comfort and public health (Watkins et al., 2007; Chan et al., 2013). In high-density urban environment, compacted building form reduces air ventilation and prevents the release of longwave radiation during night-time, leading to nocturnal UHI phenomenon. As a result, it is important to incorporate urban climate into urban planning and design framework in order to achieve a more sustainable urban environment in the next few decades.

The relationship between urban morphology and local climatic conditions has been widely studied (Eliasson, 1990/91; 1996, Golany, 1996; Chen et al., 2012; Middel et al., 2012). Research studies found that urban design parameters have significant impacts on different aspects of urban climate (Sarkar and Ridder 2011; Mouzourides et al., 2013; Yang et al., 2013). It reiterates the potential of urban planning and design in mitigating the deteriorating urban climate. Local Climate Zone (LCZ) classification system, developed by Stewart and Oke (2012), aims to characterize local surface environments with regard to their effect on local climate. The LCZs are defined as “regions of uniform surface cover, structure, material, and human activity that span hundreds of meters to several kilometers in horizontal scale” (Stewart and Oke, 2012, p.1884). Each LCZ has distinguishable physical properties which help to determine the UHI intensity between two LCZs in terms of temperature difference. Therefore, it offers an objective comparison of the climatic characteristics between different areas (Lelovics et al., 2014). The size of LCZs generally ranges from hundreds of metres to kilometres according to the homogeneity of surface characteristics. However, in high-density cities like Hong Kong, the surface environment varies considerably within short distances. It is therefore important to determine the optimal grid size for developing LCZ classes in order to accommodate such a high variability in surface environment of Hong Kong.

The present study aims to determine the optimal size of LCZs for subsequent spatial mapping in Hong Kong. A sensitivity test was conducted to compare the effect of the size on night-time air temperature (Ta) and relatively humidity (RH) in 14 study areas. Four grid sizes (500m, 400m, 300m, and 200m) were compared for their effect on the spatial average and standard deviation of Ta and RH. Ta and RH values are simulated for individual ground pixels using ENVI-met. Analysis of Variance (ANOVA) test is conducted to examine the effect of LCZ sizes and post-hoc Tukey’s test is used to find significant different pairs. The grid size determined in the present study will be subsequently used in spatial mapping of LCZs in Hong Kong. It also provides a basis for the development of potentially new LCZ classes which are specific to high-density urban environment.

## 2. Methodology

Hong Kong is located at the southern coast of China and has a sub-tropical climate with average summer air temperature ($T_a$) of 28.4°C. The city is characterized by its high-density and high-rise urban morphology. 14 study areas were selected to represent the typical high-density urban settings of Hong Kong (Fig. 1). Details of the study areas are shown in Table 1. Data of building morphology are in the form of a digital surface model and serves as the input of the subsequent ENVI-met simulation. ENVI-met simulation was performed to model $T_a$ and relative humidity (RH) for the 14 study areas under typical summer night-time conditions. Initial conditions for the ENVI-met simulation are listed in Table 2.

For each of them, four different grid sizes (200x200m, 300x300m, 400x400m and 500x500m) were tested in order to obtain the optimal size of LCZ for its application in Hong Kong. Area averages and standard deviations of modelled $T_a$ and RH were obtained and compared by using Analysis of Variance (ANOVA) for determining whether grid size has an (statistically) significant effect. Post-hoc Tukey’s test was then carried out to determine significantly different pairs of LCZ grid size. One of the most inner urban areas of Hong Kong is then used to demonstrate the development of LCZ classes with different grid sizes.

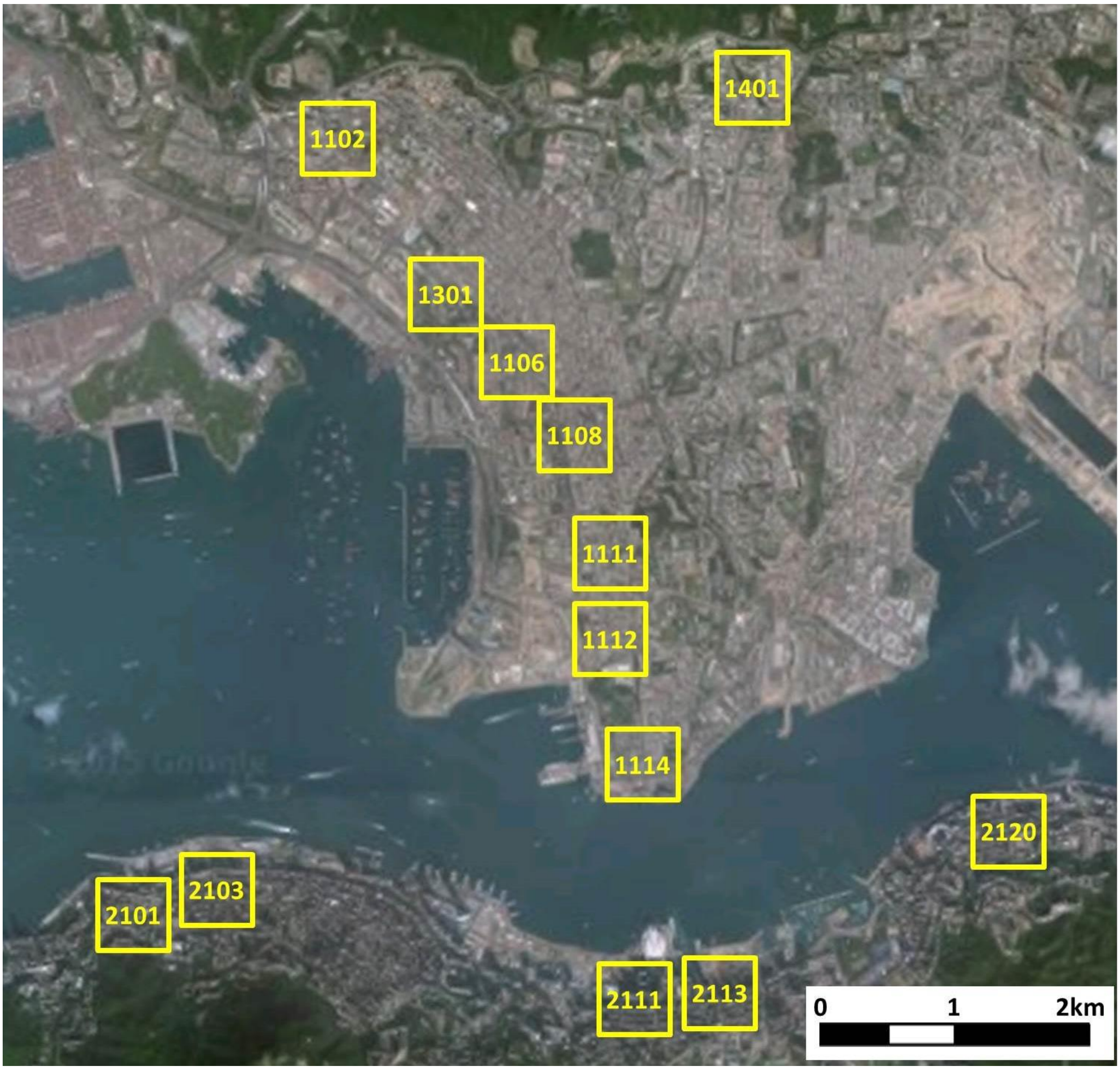

*Fig. 1 Spatial variation of LCZ classes of the Kowloon Peninsula at various grid sizes.*

*Table 1 Various urban design parameters of the study areas (MBH: Mean Building Height; SDBH: Standard Deviation of Building Height; MSVF: Mean Sky View Factor; SDSVF: Standard Deviation of Sky View Factor; BC: Building Coverage; BVD: Building Volume Density; PC: Park Coverage; SC: Street Coverage)*

| | MBH | SDBH | MSVF | SDSVF | BC | BVD | PC | SC |
|---|---|---|---|---|---|---|---|---|
| 1102 | 36.7 | 20.4 | 0.51 | 0.23 | 47.2% | 17.4 | 10.5% | 22.0% |
| 1106 | 26.5 | 13.7 | 0.44 | 0.17 | 37.8% | 10.0 | 3.9% | 34.3% |
| 1108 | 40.3 | 32.4 | 0.33 | 0.15 | 44.0% | 17.7 | 0.8% | 30.2% |
| 1111 | 31.4 | 25.1 | 0.44 | 0.20 | 38.1% | 12.0 | 2.0% | 27.7% |
| 1112 | 32.2 | 18.3 | 0.42 | 0.21 | 40.0% | 12.9 | 7.5% | 31.4% |
| 1114 | 40.4 | 33.6 | 0.45 | 0.25 | 45.7% | 18.4 | 11.0% | 23.5% |
| 1301 | 27.2 | 13.3 | 0.44 | 0.20 | 40.8% | 11.1 | 1.4% | 29.8% |
| 1401 | 19.4 | 12.3 | 0.69 | 0.21 | 21.9% | 4.3 | 9.0% | 19.8% |
| 2101 | 38.6 | 35.7 | 0.53 | 0.26 | 37.3% | 14.4 | 2.8% | 25.9% |
| 2103 | 33.4 | 29.2 | 0.44 | 0.25 | 39.2% | 13.1 | 4.2% | 32.1% |
| 2111 | 64.3 | 68.2 | 0.31 | 0.14 | 41.4% | 26.7 | 7.6% | 31.1% |
| 2113 | 54.6 | 36.6 | 0.32 | 0.16 | 38.7% | 21.1 | 1.8% | 30.3% |
| 2120 | 45.7 | 29.0 | 0.49 | 0.35 | 41.2% | 18.8 | 2.8% | 27.9% |
| 3210 | 30.1 | 22.3 | 0.64 | 0.19 | 25.0% | 7.5 | 1.4% | 22.9% |

*Table 2  Input parameters for ENVI-met simulation*

| Input Parameters | Values |
|---|---|
| Wind Speed at 10 m above Ground | 2.1 m/s |
| Wind Directions | 180° (South) |
| Roughness Length (z0) at Reference Point | 0.1 |
| Initial Air Temperature | 303.3 K |
| Specific Humidity in 2500 m | 21 g Water/kg Air |
| Relative Humidity at 2m above Ground | 79% |

## 3. Results and Discussion

### 3.1 ANOVA and Post-hoc Tukey's Test

According to the ANOVA test, there are no significant differences (α=0.05) in the area average of Ta and RH between LCZ grid sizes. However, the effect of LCZ grid sizes is found to be significant in the standard deviation of Ta and RH, suggesting that there are differences in the homogeneity of surface characteristics. Post-hoc Tukey's test also shows that 200m grid size is significantly different from the other three grid sizes except that 300m is barely different from 500m with a p-value of 0.04. It was also found that the standard deviation of both Ta and RH generally decreases with the grid size of LCZs, suggesting an increasing homogeneity of the surface environment regarding its effect on local climate.

*Table 3  ANOVA test for spatial average and standard deviation of Ta and RH*

| | | *SS* | *df* | *MS* | *F* | *Sig.* |
|---|---|---|---|---|---|---|
| Ta_Mean | Between Groups | 0.01 | 3 | 0.00 | 0.11 | 0.95 |
| | Within Groups | 1.53 | 52 | 0.03 | | |
| | Total | 1.54 | 55 | | | |
| Ta_StdDev | Between Groups | 0.04 | 3 | 0.01 | 6.77 | **0.00** |
| | Within Groups | 0.11 | 52 | 0.00 | | |
| | Total | 0.16 | 55 | | | |
| RH_Mean | Between Groups | 0.18 | 3 | 0.06 | 0.08 | 0.97 |
| | Within Groups | 39.85 | 52 | 0.77 | | |
| | Total | 40.03 | 55 | | | |
| RH_StdDev | Between Groups | 0.89 | 3 | 0.30 | 7.27 | **0.00** |
| | Within Groups | 2.12 | 52 | 0.04 | | |
| | Total | 3.01 | 55 | | | |

***Table 4.*** *Post-hoc Tukey's test for spatial average and standard deviation of Ta and RH*

| **Ta_Mean** | **500m** | **400m** | **300m** | **200m** | **Ta_StdDev** | **500m** | **400m** | **300m** | **200m** |
|---|---|---|---|---|---|---|---|---|---|
| 500m | | | | | 500m | | | | |
| 400m | 1.00 | | | | 400m | 0.71 | | | |
| 300m | 0.97 | 0.99 | | | 300m | **0.04** | 0.36 | | |
| 200m | 0.96 | 0.99 | 1.00 | | 200m | **0.00** | **0.02** | 0.46 | |

| **RH_Mean** | **500m** | **400m** | **300m** | **200m** | **RH_StdDev** | **500m** | **400m** | **300m** | **200m** |
|---|---|---|---|---|---|---|---|---|---|
| 500m | | | | | 500m | | | | |
| 400m | 1.00 | | | | 400m | 0.74 | | | |
| 300m | 0.98 | 1.00 | | | 300m | **0.04** | 0.34 | | |
| 200m | 0.97 | 0.99 | 1.00 | | 200m | **0.00** | **0.01** | 0.37 | |

### 3.2 Spatial Distribution of LCZ Classes

Figure 2 shows the spatial distribution of LCZ classes of the Kowloon Peninsula at different grid sizes. With the 400m and 500m grid sizes, the central part of the peninsula is mostly classified as compact high-rise (CH) or open high-rise (OH) while medium-rise classes dominate in the north. Increasing grid size to 300m allows a clearer picture of variations in urban morphology. For example, two linear compact high-rise areas in the central and eastern part of the peninsula are visible at 300m grid size. These areas are dominated by modern high-rise commercial and residential buildings which are densely built along main traffic routes. In addition, the medium-rise batches in the northern part of the peninsula are better distinguished into open and compact settings. It agrees with Suomi et al. (2012) that a spatial resolution of 300m is more suitable in representing floor area (i.e. building density) in the context of modelling urban heat island.

***Table 5.*** *Standard deviation of Ta and RH of the 14 study areas.*

| Ta_StdDev | 1102 | 1106 | 1108 | 1111 | 1112 | 1114 | 1301 | 1401 | 2101 | 2103 | 2111 | 2113 | 2120 | 3210 |
|---|---|---|---|---|---|---|---|---|---|---|---|---|---|---|
| 500m | 0.181 | 0.082 | 0.127 | 0.138 | 0.134 | 0.122 | 0.106 | 0.174 | 0.292 | 0.073 | 0.116 | 0.119 | 0.236 | 0.114 |
| 400m | 0.164 | 0.075 | 0.107 | 0.129 | 0.121 | 0.127 | 0.086 | 0.150 | 0.248 | 0.058 | 0.081 | 0.109 | 0.179 | 0.113 |
| 300m | 0.157 | 0.079 | 0.076 | 0.101 | 0.074 | 0.115 | 0.043 | 0.134 | 0.143 | 0.042 | 0.056 | 0.104 | 0.131 | 0.083 |
| 200m | 0.145 | 0.086 | 0.042 | 0.102 | 0.028 | 0.111 | 0.023 | 0.067 | 0.108 | 0.024 | 0.030 | 0.049 | 0.092 | 0.066 |

| RH_StdDev | 1102 | 1106 | 1108 | 1111 | 1112 | 1114 | 1301 | 1401 | 2101 | 2103 | 2111 | 2113 | 2120 | 3210 |
|---|---|---|---|---|---|---|---|---|---|---|---|---|---|---|
| 500m | 0.914 | 0.411 | 0.642 | 0.656 | 0.680 | 0.618 | 0.536 | 0.851 | 1.181 | 0.364 | 0.499 | 0.614 | 0.984 | 0.589 |
| 400m | 0.823 | 0.377 | 0.543 | 0.607 | 0.612 | 0.647 | 0.438 | 0.741 | 1.035 | 0.289 | 0.368 | 0.563 | 0.837 | 0.570 |
| 300m | 0.786 | 0.397 | 0.381 | 0.520 | 0.373 | 0.587 | 0.217 | 0.667 | 0.622 | 0.211 | 0.259 | 0.534 | 0.664 | 0.427 |
| 200m | 0.726 | 0.432 | 0.211 | 0.526 | 0.142 | 0.561 | 0.117 | 0.341 | 0.500 | 0.119 | 0.143 | 0.250 | 0.466 | 0.373 |

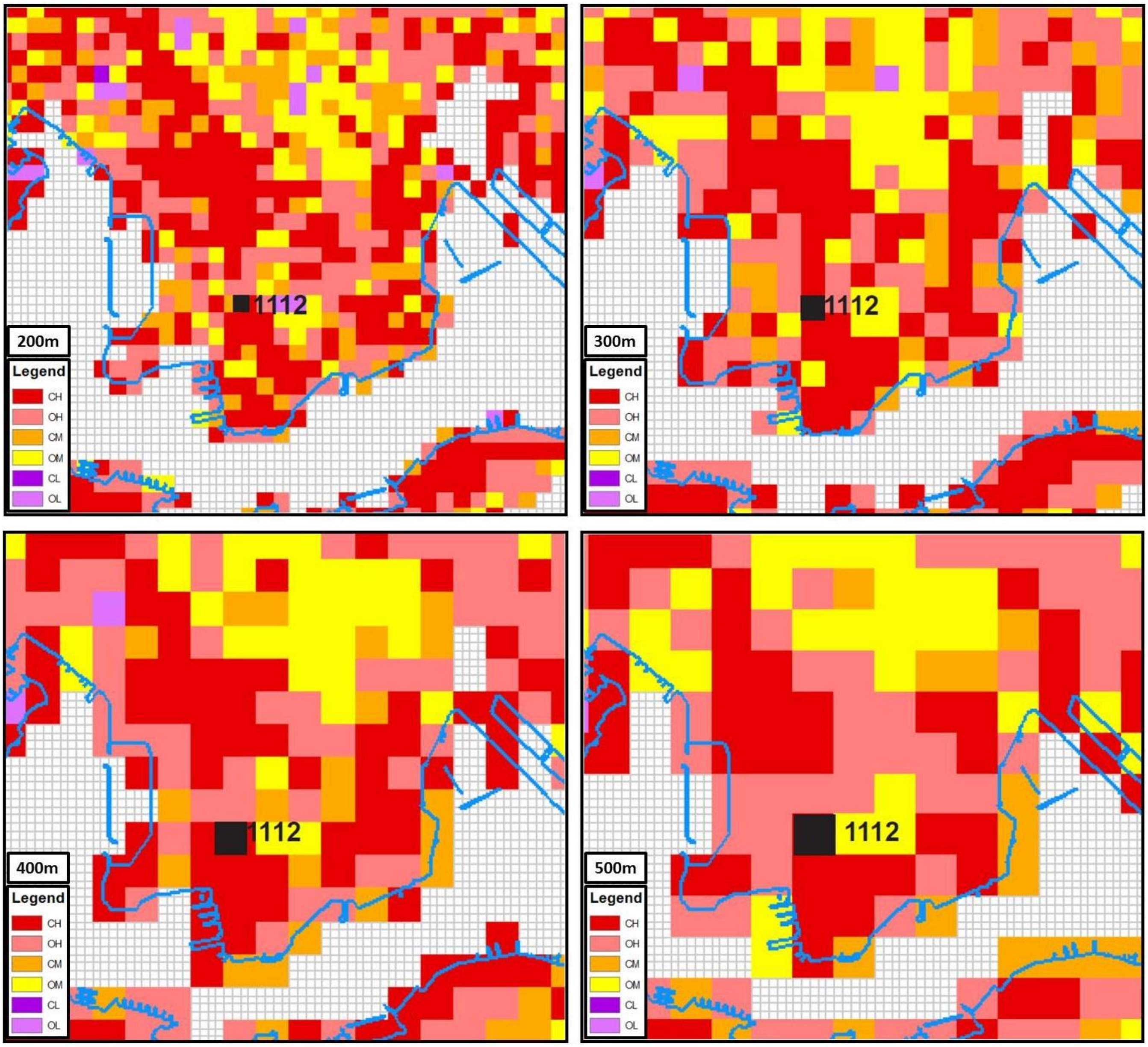

*Fig. 2 Spatial variation of LCZ classes of the Kowloon Peninsula at various grid sizes.*

At a spatial resolution of 200m, the intra-urban differences in urban morphology and surface characteristics are described in more details. The OH area in the central part of the peninsula depicts the limitations of topography which allows only urban development with relatively open settings. In the northern part of the peninsula, medium-rise residential areas become more visible while occasional open low-rise areas are scattered within the medium-rise batches. In addition, a finer resolution would help to define potential air paths at city scale (Yuan et al., 2014), which are particularly important to coastal cities like Hong Kong since sea breezes are one of the key mitigation elements to urban heat island.

## 4. Future Development

An appropriate grid size is very important to the spatial mapping of urban climatic conditions and urban morphology since increasing spatial resolution only would result in high computational time and complexities for the urban planning and design practitioners while low spatial resolution is not capable of capturing the intra-urban differences or heterogeneities. The present study proposes a grid size of 300m for the spatial mapping of LCZs in Hong Kong and further development of new LCZ classes for high-density cities. Grid size of 200m may also be considered for identifying ventilation paths at district level. The validity of the grid size will be enhanced by defining the relationship between urban heat island intensity and various urban design parameters. Spatial pattern of LCZ classes for individual districts will have to be carefully examined. Further field measurements will also be required in order to validate the development of LCZs in such a high-density urban environment.

## Acknowledgment

This study is sponsored by the Research Grants Council of Hong Kong (Project No.: RGC-ECS458413) and Social Science Seed Grant of Faculty of Social Science of CUHK (Project title: Studying the urban climate in a high-density city in typical summer days; project code: 6903791). The authors wish to extend sincere thanks to Mr. LEE Max and Mr. LUI Fung Wai of The Chinese University of Hong Kong for their support in the traverse measurements.

## References

Chan EYY., Goggins W.B., Yue J.S.K., Lee P., 2013: Hospital admissions as a function of temperature, other weather phenomena and pollution levels in an urban setting in China. *Bulletin of the World Health Organization*, **91(8)**, 576–584.

Eliasson I., 1990/91: Urban geometry, surface temperature and air temperature. *Energy Buildings*, **15–16**, 141–145.

Eliasson I., 1996: Urban nocturnal temperatures, street geometry and land use. *Atmospheric Environment*, **30**, 379–392.

Giridharan R., Ganesan S., Lau S.S.Y., 2004: Daytime urban heat island effect in high-rise and high-density residential developments in Hong Kong. *Energy and Buildings*, **36(6)**, 525–534.

Golany G.S., 1996: Urban design morphology and thermal performance. *Atmospheric Environment*, **30**, 455–465.

Lau S.S.Y., Yang F., Tai J, Wu X.L., Wang J., 2011: The study of summer-time heat island, built form and fabric in a densely built urban environment in compact Chinese cities: Hong Kong, Guangzhou. *International Journal of Sustainable Development*, **14(1-2)**, 30–48.

Middel A., Brazel A.J., Gober P., Myint S.W., Chang H., Duh J.D., 2012: Land cover, climate, and the summer surface energy balance in Phoenix, AZ, and Portland, OR. *International Journal of Climatology*, **32(13)**, 2020–2032.

Mouzourides P., Kyprianou A., Neophytou M.K.A., 2013: A scale-adaptive approach for spatially-varying urban morphology characterization in boundary layer parametrization using multi-resolution analysis. *Boundary-Layer Meteorology*, **149**, 455–481.

Oke T.R., 1982: The energetic basis of the urban heat island. *Quarterly Journal of Royal Meteorological Society*, **108**, 1–24.

Oke T.R., 1987: *Boundary-layer Climate*. Routledge, London.

Sarkar A., De Ridder K., 2011: The urban heat island intensity of paris: A case study based on a simple urban surface parametrization. *Boundary-Layer Meteorology*, **138**, 511–520.

Suomi J., Hjort J., Kayhko J., 2012: Effects of scale on modelling the urban heat island in Turku, SW Finland. *Climate Research*, **55**, 105–118.

Watkins R., Palmer J., Kolokotroni M., 2007: Increased temperature and intensification of the urban heat island: implications for human comfort and urban design. *Built Environment*, **33(1)**, 85–96.

Yang F., Qian F., Lau S.S.Y., 2013: Urban form and density as indicators for summertime outdoor ventilation potential: A case study on high-rise housing in Shanghai. *Building and Environment*, **70**, 122–137.

Yuan C., Ren C., Ng E., 2014: GIS-based surface roughness evaluation in the urban planning system to improve the wind environment – A study in Wuhan, China. *Urban Climate*, **10(3)**, 585–593.